

Wire electric discharge machining characteristics of titanium nickel shape memory alloy

M. MANJIAH¹, S. NARENDRANATH¹, S. BASAVARAJAPPA², V. N. GAITONDE³

1. Department of Mechanical Engineering, National Institute of Technology, Surathkal, Karnataka, India;

2. Department of Studies in Mechanical Engineering, University B.D.T. College of Engineering, Davangere-577 004, Karnataka, India;

3. Department of Industrial and Production Engineering, B. V. B. College of Engineering and Technology, Hubli-580 031, Karnataka, India

Received 29 November 2013; accepted 15 March 2014

Abstract: TiNi shape memory alloys (SMAs) have been normally used as the competent elements in large part of the industries due to outstanding properties, such as super elasticity and shape memory effects. However, traditional machining of SMAs is quite complex due to these properties. Hence, the wire electric discharge machining (WEDM) characteristics of TiNi SMA was studied. The experiments were planned as per L_{27} orthogonal array to minimize the experiments, each experiment was performed under different conditions of pulse duration, pulse off time, servo voltage, flushing pressure and wire speed. A multi-response optimization method using Taguchi design with utility concept has been proposed for simultaneous optimization. The analysis of means (ANOM) and analysis of variance (ANOVA) on signal to noise (S/N) ratio were performed for determining the optimal parameter levels. Taguchi analysis reveals that a combination of 1 μ s pulse duration, 3.8 μ s pulse off time, 40 V servo voltage, 1.8×10^5 Pa flushing pressure and 8 m/min wire speed is beneficial for simultaneously maximizing the material removal rate (MRR) and minimizing the surface roughness. The optimization results of WEDM of TiNi SMA also indicate that pulse duration significantly affects the material removal rate and surface roughness. The discharged craters, micro cracks and recast layer were observed on the machined surface at large pulse duration.

Key words: TiNi shape memory alloy; wire electric discharge machining (WEDM); surface roughness; material removal rate; surface morphology

1 Introduction

Titanium nickel (TiNi) shape memory alloy (SMA) has maximum recoverable strain up to 8% compared with other SMAs, and hence finds broad applications in actuators, vibration and seismic absorbers [1], orthodontic springs [2], endovascular stents [3] and coupling systems for pipes [4]. TiNi is one of the most important biomaterials used in the field of medical applications due to its biocompatibility, better corrosion resistance, superelasticity and shape memory effect (SME). However, the development of this material causes difficulties in manufacturing process. The conventional machining of TiNi SMAs is very difficult due to poor thermal conductivity. Because of lower thermal conductivity, the generated heat is concentrated on the tool tip, leading to higher tool wear, severe strain

hardening, high toughness and viscosity and unique property of super elastic behavior [5,6]. To overcome these difficulties, special machining techniques, such as electric discharge machining (EDM) [7], wire electric discharge machining (WEDM) [8] and laser machining [9] have been performed for machining TiNi alloys.

Presently, WEDM is a prevalent technique, which is typically suitable for precision engineering applications of conductive materials. During WEDM, the damaging impacts on surface integrity of machined surface, such as craters, micro voids, recast layer and heat affected zone, are agreeable for cracking and reduction in fatigue strength [10]. Improving the surface quality and property by decreasing the formations of recast layer, cracks, oxides and carbide on machined surface can be achieved using optimal WEDM process parameters. Reduction in surface roughness can improve the fatigue strength, corrosion and wear resistance of the material [11].

The discharge current and pulse duration are the most significant parameters influencing the material removal rate and surface roughness. Optimum process parameter is crucial to reduce the machining cost and to machine intricate shapes with enhanced surface property [12]. FAN et al [13] developed a multi precision pulse power based micro controller unit to adjust the electric parameters. They reported that the best surface finish could be achieved by constant pulse interval and pulse duration with proper selecting capacitance. SELVAKUMAR et al [14] analysed the corner accuracy in WEDM of Monel 400 alloy. The studies indicated that the corner accuracy was more or less independent of sparking factors and primarily influenced by flushing height, job height and corner angle. Multi objective optimization in WEDM of Ti6242 alloy was performed by GARG et al [15] by integrating Box-Behnken design with genetic algorithm (GA). Recently, the machinability study in EDM of TiNi SMA has been carried out by ALIDOOSTI et al [7]. They found that the recast layer formed during machining, leading to higher surface hardness of the material. PROHASZKA et al [16] reported that the machining speed increased, primarily due to the presence of zinc in wire electrode.

Although some studies have been reported in the literatures on machining of TiNi SMA, no systematic work has been carried out to optimize the process parameters in WEDM of TiNi SMA. This work demonstrates the application of Taguchi method with the utility concept for multi-objective WEDM process optimization. The key advantage of Taguchi technique is that the method allows the process optimization with minimum number of experiments without the need for process model development [17,18]. Thus, by this method, it is possible to reduce the time and cost for experimental investigations and improve the performance characteristic with minimum experiments. Taguchi optimization technique is based on the concept of “robust design”, which aims at obtaining the solutions that make the designs less sensitive to the noise factors. Taguchi methods have been extensively applied in the process design, wherein the mathematical models for performance do not exist and the experiments are typically conducted to determine the optimum settings for design and process variables. However, Taguchi method is applied for a single performance characteristic, and hence several modifications were suggested to improve the original Taguchi method for multi response optimization [19]. The utility concept [20] employs the weighting factors to each of the signal to noise (S/N) ratio of the performance characteristics to acquire a multi-response S/N ratio for each trial of the orthogonal array (OA). In the present research work, the modified Taguchi method was used to find out the optimal process

parameters, namely, pulse duration, pulse off time, servo voltage, flushing pressure and wire speed, to simultaneously optimize the material removal rate and surface roughness of workpiece during WEDM of TiNi SMA. Further, the surface morphology, recast layer, machined surface hardness and microstructure were also investigated.

2 Experimental

2.1 Taguchi method with utility concept

Taguchi method is used to find the optimum setting of control factors to make the product or process insensitive to noise factors. Taguchi design is based upon the technique of matrix experiments, known as orthogonal arrays [17,18], which allow the simultaneous effect of numerous factors to be studied proficiently. Taguchi method suggests signal to noise (S/N) ratio as the objective function for matrix experiments [17,18]. Taguchi method classifies objective functions into three categories, namely, smaller the better type, larger the better type and nominal the best type. The optimum level for a factor is the level that results in the highest S/N ratio value in the experimental region.

Taguchi technique with utility concept [20,21] involves assigning a weight for each performance characteristic. A weight to each S/N ratio of the characteristic is assigned and the weighted S/N ratio is summed for computing the performance of a multi-objective problem. If X_i is a measure of effectiveness of an attribute i and there are n attributes evaluating the outcome space, then the overall utility function is given by

$$U(X_1, X_2, \dots, X_n) = \sum_{i=1}^n U_i(X_i) \quad (1)$$

where $U_i(X_i)$ is the utility of the i th attribute. Depending on the requirements, the attributes may be given priorities and weights. Hence, the weighted form of Eq. (1) is as follows:

$$U(X_1, X_2, \dots, X_n) = \sum_{i=1}^n w_i U_i(X_i) \quad (2)$$

where $\sum_{i=1}^n w_i = 1$; w_i is the weight assigned to attribute i .

2.2 Workpiece material

The workpiece material used in the present investigation is Ti₅₀Ni₅₀ SMA specimen. Pure metal pieces from titanium rods containing 99% titanium (mass fraction) and nickel rods containing 99% nickel were mixed with equal mass (about 10 g) into copper mould melting chamber under vacuum. Prior to melting, the

chamber was pumped out and subsequently filled with high purity argon gas. The melting temperature was around 1500 °C. The alloys were melted and remelted six times into buttons for homogeneity. The buttons were then cast into rods of each 4 mm in diameter and 70 mm in height. The scanning electron microscopy (SEM) equipped with energy dispersive X-ray spectrometry (EDS) unit is used to study the melted alloy elemental composition. Figure 1 shows the EDS analysis of cast TiNi alloy.

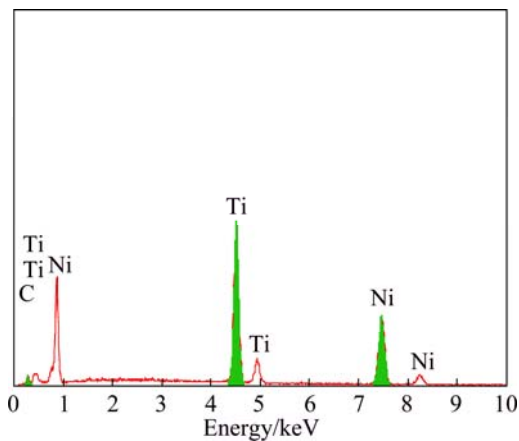


Fig. 1 EDS analysis of cast TiNi alloy

2.3 Experimental details

In the current research, five parameters, namely, pulse duration, pulse off time, servo voltage, flushing pressure and wire speed, were identified. The range of the each parameter was determined from the preliminary experiments. Each process parameter was investigated at three levels to study the non-linearity effect of the parameters. The identified controllable parameters in WEDM of TiNi SMA experiments and their associated levels are listed in Table 1. Table 2 shows the machining parameters, which are kept constant throughout the investigation.

Table 1 Controllable parameters and their levels

Code	Parameter	Level 1	Level 2	Level 3
A	Pulse duration/ μs	0.2	0.6	1
B	Pulse off time/ μs	3.8	14	25
C	Servo voltage/V	20	40	60
D	Flushing pressure/Pa	1.8×10^5	2.3×10^5	3.3×10^5
E	Wire speed/($\text{m} \cdot \text{min}^{-1}$)	2	8	14

Table 2 Fixed machining parameters

Machining parameter	Value
Pulse current/A	14
Short pulse time/ μs	0.2
Wire mechanical tension/daN	1

It has been reported that material removal rate is higher in deionized water dielectric fluid compared with kerosene. And more oxides and carbides were also formed during usage of kerosene and additive fluids compared with deionized water [22]. Hence, deionized water was used as the dielectric fluid in the current investigation. The brass wire possesses reasonable conductivity with high tensile strength when compared with the copper wire in addition to favorable properties, availability and the low cost [23]. Hence, the brass wire of 0.25 mm in diameter was selected as electrode, which consisted of 65% zinc and 35% copper.

The experiments were performed on Robofill–290 WEDM machine (Charmills Co.) as per L_{27} orthogonal array. The experimental layout plan is listed in Table 3. The photographs of as-cast TiNi SMA alloy rod (workpiece) and the experimental setup used in the present experimentation are shown in Fig. 2.

2.4 Measurement

The machining time was determined using stopwatch. The material removal rate (MRR) is calculated as follows:

$$r = \frac{V}{t} = \frac{W}{dt} \quad (4)$$

where r is the MRR; V is the volume of material removed; t is the machining time; W is the workpiece removal weight; d is the density of workpiece.

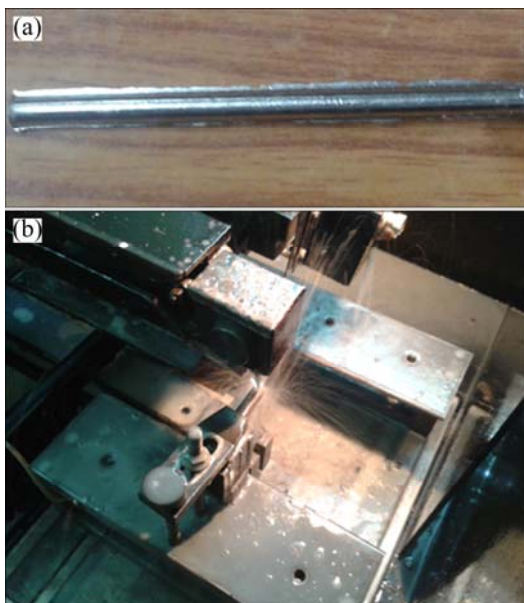
The surface roughnesses of WEDMed surfaces were measured using Mitutoyo surface roughness tester. The average surface roughness (R_a), which was commonly used in the manufacturing industry, was considered for the current study. The surface roughness of the workpiece was measured at three different locations and the average was taken as the process response. The cutoff length selected for the measurement of surface roughness is 4 mm at a stylus speed of 0.25 mm/s.

The measured values of surface roughness (R_a) and computed values of material removal rate for the current investigation are listed in Table 3.

The surface microhardness was measured using a microhardness tester under the condition of 245 mN load and 13 s dwell time. Moreover the 3D surface morphology measurement device (confocal instrument with LEXT analysing software at CMTI, Bangalore, India) was used to observe the WEDMed 3D surface morphology of TiNi SMA samples. The scanning electron microscopy and energy dispersive X-ray spectrometer were used to study the morphology and elemental composition of WEDMed samples. The X-ray diffraction analyzer (BRUKER D8 Advance) was carried out to investigate the microstructural feature and phases of WEDMed samples.

Table 3 Experimental plan with responses, corresponding S/N ratios and multi-response S/N ratio

Trial No.	Level of process parameter setting					$r/(\text{mm}^3 \cdot \text{min}^{-1})$	Response Surface roughness, $R_a/\mu\text{m}$	S/N ratio		
	A	B	C	D	E			η_1	η_2	η
1	1	1	1	1	1	1.55515	2.021	3.8354	-6.1113	-1.1379
2	1	1	1	1	2	2.03987	1.742	6.192	-4.821	0.6855
3	1	1	1	1	3	2.61783	1.395	8.3588	-2.8915	2.7337
4	1	2	2	2	1	0.77184	1.91	-2.2495	-5.6207	-3.935
5	1	2	2	2	2	1.16348	1.481	1.3152	-3.4111	-1.048
6	1	2	2	2	3	1.64471	1.963	4.3218	-5.8584	-0.7683
7	1	3	3	3	1	0.91945	3.223	-0.7294	-10.1652	-5.4473
8	1	3	3	3	2	0.59836	2.039	-4.4607	-6.1883	-5.3245
9	1	3	3	3	3	0.86698	2.083	-1.2398	-6.3738	-3.8068
10	2	1	2	3	1	4.68866	1.871	13.421	-5.4415	3.9897
11	2	1	2	3	2	6.11882	1.312	15.7334	-2.3587	6.6873
12	2	1	2	3	3	5.09471	1.608	14.1424	-4.1257	5.0083
13	2	2	3	1	1	3.95941	1.689	11.9526	-4.5526	3.7
14	2	2	3	1	2	4.50962	1.377	13.0828	-2.7787	5.1521
15	2	2	3	1	3	5.12129	1.722	14.1876	-4.7207	4.7335
16	2	3	1	2	1	4.28334	1.894	12.6357	-5.5476	3.544
17	2	3	1	2	2	4.4458	1.813	12.959	-5.168	3.8955
18	2	3	1	2	3	4.20761	1.736	12.4807	-4.791	3.8449
19	3	1	3	2	1	7.92083	2.105	17.9754	-6.465	5.7552
20	3	1	3	2	2	7.8535	2.224	17.9013	-6.9427	5.4793
21	3	1	3	2	3	7.03404	2.112	16.9441	-6.4939	5.2251
22	3	2	1	3	1	4.8825	1.89	13.7728	-5.5292	4.1218
23	3	2	1	3	2	3.84693	1.624	11.7023	-4.2117	3.7453
24	3	2	1	3	3	3.50368	1.476	10.8905	-3.3817	3.7544
25	3	3	2	1	1	8.56901	2.017	18.6586	-6.0941	6.2822
26	3	3	2	1	2	8.64447	1.553	18.7348	-3.8234	7.4557
27	3	3	2	1	3	8.34148	2.471	18.4249	-7.8575	5.2837

**Fig. 2** Optical images of as-cast TiNi SMA alloy rod (a) and aspect of machining process (b)

3 Results and discussion

3.1 ANOM and ANOVA

The analysis of means (ANOM) on signal to noise (S/N) ratio was performed for determining the optimal parameter levels. In the present study, Taguchi design with utility concept is proposed for optimizing the multiple responses, i.e. r and R_a . Here, r is to be maximized and R_a is to be minimized. Hence “larger the better type” characteristic for r and “smaller the better type” characteristic for R_a have been selected. The S/N ratios associated with the responses are given as follows:

$$\eta_1 = -10 \lg \frac{1}{r^2} \quad (5)$$

$$\eta_2 = -10 \lg R_a^2 \quad (6)$$

In the utility concept, the multi-response S/N ratio is given by GAITONDE et al [21] as follows:

$$\eta = w_1 \eta_1 + w_2 \eta_2 \quad (7)$$

where w_1 and w_2 are the weighting factors associated with S/N ratio for each of the machining characteristics, r and R_a , respectively. In the present study, weighting factor of 0.5 for each of the machining characteristics is considered, which gives equal priorities to both r and R_a for simultaneous optimization. The calculated values of S/N ratio for each characteristic and the multi-response S/N ratio for each trial in the orthogonal array are listed in Table 3.

Analysis of means (ANOM) was used to determine the optimum levels of the process parameters. The ANOM results are listed in Table 4 and the optimal combination of process parameters for simultaneously optimizing surface roughness and material removal rate is A3, B1, C2, D1 and E2. Hence, a combination of 1 μ s pulse duration, 3.8 μ s pulse off time, 40 V servo voltage, 1.8×10^5 Pa flushing pressure and 8 m/min wire speed is beneficial for simultaneously maximizing the material removal rate and minimizing the surface roughness.

Table 4 ANOM based on S/N ratio

Parameter code	Level 1	Level 2	Level 3	Optimum level
A	-2.0054	4.5062	5.2336	3
B	3.8251	2.1617	1.7475	1
C	2.7986	3.2173	1.7185	2
D	3.8765	2.4436	1.4142	1
E	1.8747	2.9698	2.8898	2

The relative importance of the control factors was investigated through the analysis of variance (ANOVA). Table 5 lists the summary of ANOVA results. It is found that the pulse duration has the highest contribution (77.53%) followed by flushing pressure and pulse off time. However, servo voltage and wire speed have the least effects in optimizing the multi-performance characteristics in WEDM of TiNi SMA. It is revealed that the pulse duration is the major influencing parameter

Table 5 ANOVA results based on S/N ratio

Parameter code	Degree of freedom	Sum of square	Mean square	Contribution/%
A	2	286.0000	143.0000	77.53
B	2	21.7655	10.8827	5.90
C*	2*	10.7650 *	5.3825	2.92
D	2	27.5261	13.7631	7.46
E*	2*	6.7077*	3.3539	1.82
Error	16	16.1098	0.6531	4.37
Total	26	368.8742	14.1875	100
Poole error	20	33.5826	1.6791	

*pooled

on both r and R_a . This means that the pulse duration is higher, the discharge energy and intensity of spark will be greater, which will remove larger chunk of material and form a deeper and larger crater, leading to higher r and R_a . The dominant factors of controlling the energy input are the pulse duration and pulse off time. A shorter pulse off time causes larger number of sparks discharge in a given time, which helps to remove material at faster rate [15].

The confirmation experiments were conducted at the optimal process parameter levels (A3, B1, C2, D1 and E2). Three trials were conducted and the corresponding surface roughness values were measured and the r values were computed. The results of the confirmatory experiments are listed in Table 6. It is found that the prediction error is within the 95% confidence interval and hence justifying the adequacy of the additivity of the model.

Table 6 Results of confirmatory experiments

Predicted S/N ratio	Observed S/N ratio	Predicted error
7.7790	7.5025	0.0355

3.2 Surface morphology analysis

3D surface morphology of machined surface was measured using confocal microscope. The Japan electro-optics laboratory (JEOL) scanning electron microscope was used to examine the surface micrograph. Figure 3 shows the 3D morphologies and SEM images of WED-machined samples of TiNi SMA. The peaks and valleys were observed from the morphology and the agglomerated globules of debris were seen in SEM images, primarily due to the random distribution of sparks on the machined surface.

In this process, the material is removed by melting and evaporation and then forms craters on the machined surface. Figures 3(a) and (b) show the machined condition at higher wire speed (14 m/min) with remaining all the other parameters at lower level (Trial No. 3 of Table 3). The surface shows the coral reef microstructure and the melted material droplets of uneven structure orientation, yielding a rough surface and r of 2.617 mm^3/min . As can be seen from Figs. 3(c) and (d), the surface morphology seems a greenish and blueish surface of greater peaks and valleys; uneven surface, pockmarks and pits also appear (Trial No. 27 in Table 3). At this machining condition, the surface roughness is 2.47 μm and r is 8.341 mm^3/min . This is because of longer pulse duration, pulse off time and greater wire speed. Therefore, the molten material is splashed around the surface by flushing pressure. Micro voids are also formed on the machined surface because

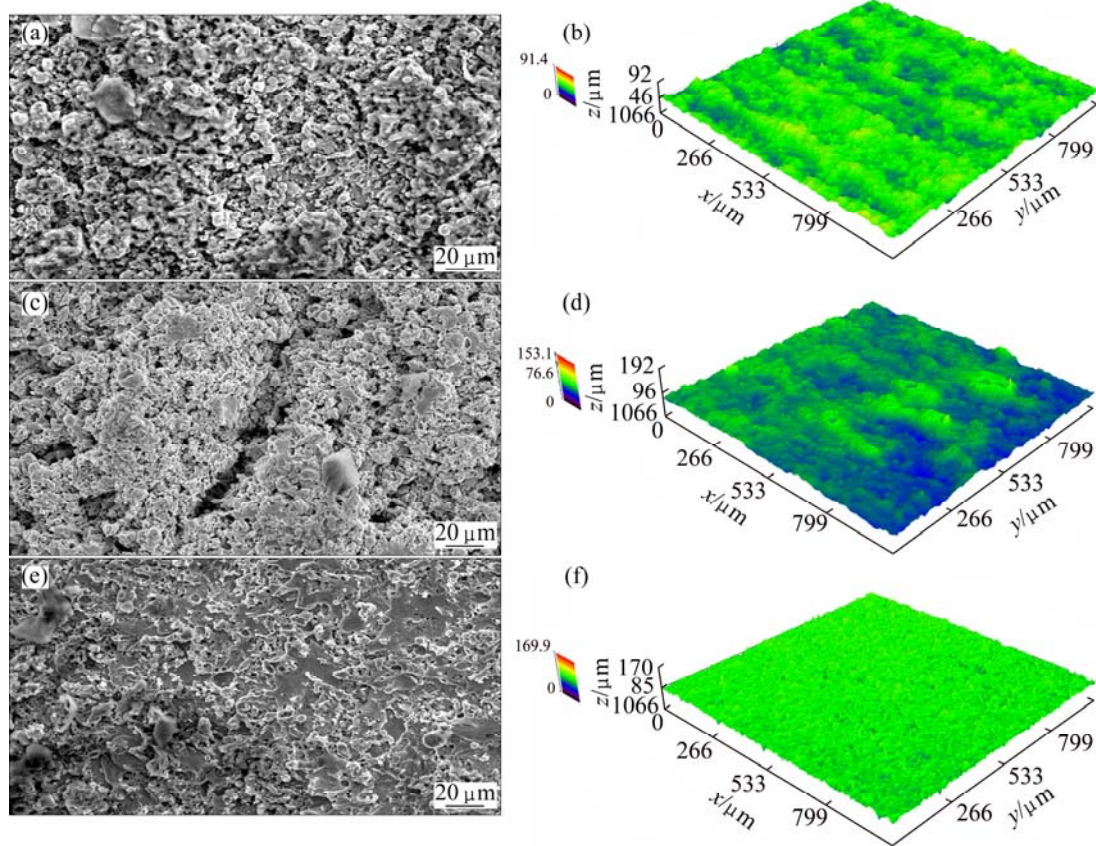


Fig. 3 SEM images and 3D surface morphologies of machined surface: (a, b) Trial No. 3; (c, d) Trial No. 27; (e, f) Optimal process parameter combination (A3, B1, C2, D1, E2)

of discharge of large volume of gases in channel, which spill out from the molten pool. Figures 3(e) and (f) show the machined surface at optimal process parameter condition. The better surface quality is observed along with the redeposition of the material on the machined surface, mostly due to higher pulse duration along with slower wire speed, which clearly justifies the application of Taguchi approach with utility concept in WEDM of TiNi SMA.

3.3 Energy dispersive X-ray (EDAX) analysis

Figures 4(a) and (b) show the EDAX analysis of machined surface at the combination of higher pulse duration (1 μ s), pulse off time (25 μ s), servo voltage (40 V), flushing pressure (1.8×10^5 Pa) and wire speed (14 m/min). The elemental analysis studied the surface characteristics of WEDMed surface on the machined surface. The temperature of the discharge spark is around 10000–12000 $^{\circ}$ C. It is observed that the harder surface is formed by the chemical reaction among the work material, wire material and deionized water. Brass wire is disassociated into Cu and Zn, which reacts with the oxygen from the distilled water and forms Cu_2O and ZnO_2 . The distilled water dissociates into hydrogen and oxygen reacting with titanium and it forms TiO_2 due to

high discharge energy on the workpiece material, leading that more heat energy and non uniform cooling and heating by the longer pulse off time causes for greater surface oxidation [10]. This oxides are the cause for the increase in the machined surface hardness. Figures 4(c) and (d) show that the cross section image of WEDMed TiNi alloy at longer pulse off time and the formation of white layer is clearly observed on the machined surface (around 11 μ m). The quantitative analysis of the white layer is done by EDAX analysis, showing that the white layer is covered with carbon (71.55%) and oxygen (28.45%) content. This indicates that the surface is oxidized and carbonized.

3.4 Microhardness analysis

Figure 5 shows the microhardnesses at various distances from the edge surface up to a depth of 120 μ m under the testing conditions of 245 mN load and 13 s dwell time. The machined surface hardness at higher pulse duration (Trial No. 27 in Table 3) is varied up to a depth of 100 μ m. It is seen that the surface layer is altered up to a depth of 100 μ m because of quenching effect from the dielectric fluid and the formation of oxides and carbides on the machined surface. This effect is also due to the disassociation of brass electrode and

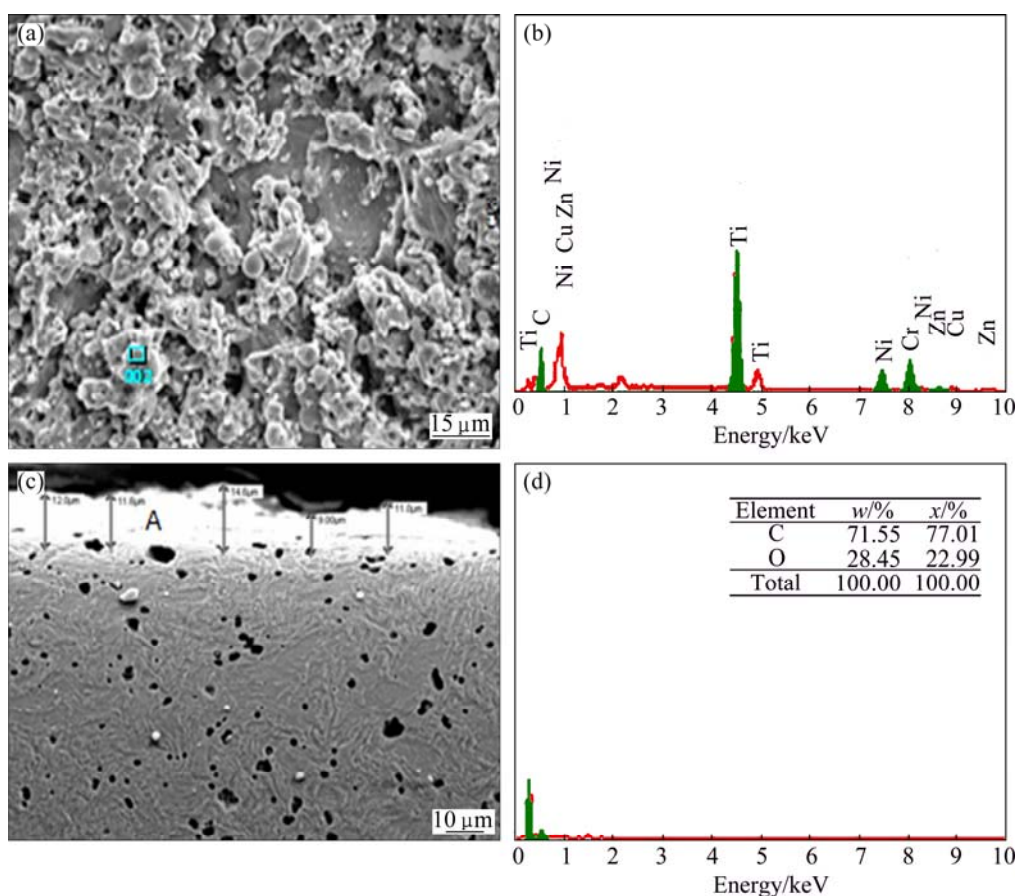


Fig. 4 SEM image (a) and EDX analysis (b) of machined surface, SEM image (c) and EDX analysis (b) of cross sectioned machined surface at high pulse duration (Trial No. 27)

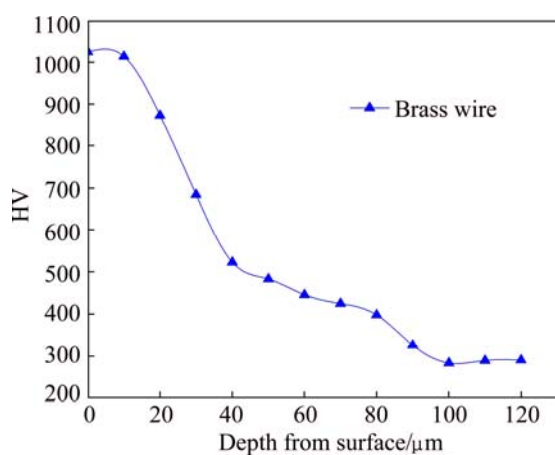


Fig. 5 Cross sectioned microhardness from machine surface (Trial No. 27)

distilled water at higher temperatures. The brass electrode contains copper and zinc, which reacts with the titanium and nickel, and forms Ni_3ZnC , CuZn , NiZn , Cu_2NiZn , CuTi , Ni_3ZnC and Ni_4Ti_3 . The distilled water may also react with copper and titanium to form Cu_2O , TiO_2 and TiNiO_3 , which is clearly evidenced in EDAX peak (Fig. 4(b)). The formation of the alloy compounds observed from the XRD analysis is shown in Fig. 6,

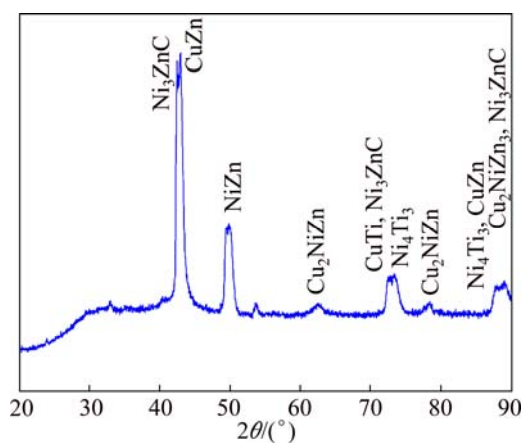


Fig. 6 XRD pattern of WEDMed surface layer for $\text{Ti}_{50}\text{Ni}_{50}$ (pulse duration of 1 μs , pulse off time of 25 μs , servo voltage of 40 V, flushing pressure of 1.8×10^5 Pa, wire speed of 14 m/min)

which is due to the formation of phases, which in turn causes higher surface hardness. Alloying element of the wire vaporizes and penetrates into the workpiece surface, which causes a phase change on the machined surface compared with the substrate TiNi alloy. The existence of these compounds changes mechanical properties of

machined surface up to 100 μm . These findings also support the investigations carried out by ALIDOOSTI et al [7].

4 Conclusions

1) The optimization of machining parameters to determine the optimal values of pulse duration, pulse off time, servo voltage, flushing pressure and wire speed for simultaneously minimizing the surface roughness and maximizing the material removal rate was carried out using Taguchi approach with utility concept. The experiments were planned as per L_{27} orthogonal array to minimize the experiments.

2) The pulse duration is the most significant parameter followed by flushing pressure and pulse off time. The servo voltage and wire speed do not have any significant effects on optimizing the multiple performances.

3) The peaks and valleys were observed by the 3D surface morphology and the agglomerated globules of debris were seen by SEM.

4) The white layer formation was observed on the machined surface at larger pulse off time.

5) The formation of the alloy compounds observed from the XRD analysis is due to the formation of phases, which in turn causes higher surface hardness.

References

- [1] SAADAT S, SALICHS J, NOORI M, HOU Z, DAVOODI H, BAR-ON I, SUZUKI Y, MASUDA A. An overview of vibration and seismic applications of NiTi shape memory alloy [J]. *Smart Materials and Structures*, 2002, 11: 218–229.
- [2] WICHELHAUS A, BRAUCHLI L, BALL J, MERTMANN M. Mechanical behavior and clinical application of nickel-titanium closed-coil springs under different stress levels and mechanical loading cycles [J]. *American Journal of Orthodontics and Dentofacial Orthopedics*, 2010, 137(5): 671–678.
- [3] STOECKEL D, PELTON A, DUERIG T. Self-expanding nitinol stents: Material and design considerations [J]. *European Radiology*, 2004, 14: 292–301.
- [4] MALETTA C, FILICE L, FURGIUELE F. NiTi Belleville washers: Design, manufacturing and testing [J]. *Journal of Intelligent Material Systems and Structures*, 2013, 24(6): 695–703.
- [5] WEINERT K, PETZOLDT V. Machining of NiTi based shape memory alloys [J]. *Materials Science and Engineering A*, 2004, 378(1–5): 180–184.
- [6] LIN H C, LIN K M, CHEN Y C. A study on the machining characteristics of TiNi shape memory alloys [J]. *Journal of Materials Processing Technology*, 2000, 105(3): 327–332.
- [7] ALIDOOSTI A, GHAFARI-NAZARI A, MOZTARZADEH F, JALALI N, MOZTARZADEH S, MOZAFARI M. Electrical discharge machining characteristics of nickel–titanium shape memory alloy based on full factorial design [J]. *Journal of Intelligent Material Systems and Structures* 2013, 24(13): 1546–1556.
- [8] HSIEH S F, CHEN S L, LIN H C, LIN M H, CHIOU S Y. The machining characteristics and shape recovery ability of Ti–Ni–X ($X=\text{Zr,Cr}$) ternary shape memory alloys using the wire electro-discharge machining [J]. *International Journal of Machine Tools and Manufacture*, 2009, 49(6): 509–514.
- [9] PFEIFER R, HERZOG D, HUSTEDT M, BARCIKOWSKI S. Pulsed Nd:YAG laser cutting of NiTi shape memory alloys—Influence of process parameters [J]. *Journal of Materials Processing Technology*, 2010, 210(14): 1918–1925.
- [10] KURIAKOSE S, SHUNMUGAM M S. Characteristics of wire-electro discharge machined Ti6Al4V surface [J]. *Materials Letters*, 2004, 58(17–18): 2231–2237.
- [11] DANESHMAND S, HESSAMI R, ESFANDIAR H. Investigation of wire electro discharge machining of nickel–titanium shape memory alloys on surface roughness and MRR [J]. *Life Science Journal*, 2012, 9: 2904–2909.
- [12] RAO R V, PAWAR P J. Modelling and optimization of process parameters of wire electrical discharge machining [J]. *Proceedings of the Institution of Mechanical Engineers, Part B: Journal of Engineering Manufacture*, 2009, 223(11): 1431–1440.
- [13] FAN Y, BAI J, LI C, XU W. Research on precision pulse power technology of WEDM [J]. *Procedia CIRP*, 2013, 6: 268–274.
- [14] SELVAKUMAR G, SARKAR S, MITRA S. Experimental investigation on die corner accuracy for wire electrical discharge machining of Monel 400 alloy [J]. *Proceedings of the Institution of Mechanical Engineers, Part B: Journal of Engineering Manufacture*, 2012, 226(10): 1694–1704.
- [15] GARG M P, JAIN A, BHUSHAN G. Modelling and multi-objective optimization of process parameters of wire electrical discharge machining using non-dominated sorting genetic algorithm-II [J]. *Proceedings of the Institution of Mechanical Engineers, Part B: Journal of Engineering Manufacture*, 2012, 226(12): 1986–2001.
- [16] PROHASZKA J, MAMALIS A G, VAXEVANIDIS N M. The effect of electrode material on machinability in wire electro-discharge machining [J]. *Journal of Materials Processing Technology*, 1997, 69(1–3): 233–237.
- [17] PHADKE M S. *Quality engineering using robust design* [M]. New Jersey: Prentice Hall, 1989.
- [18] ROSS P J. *Taguchi techniques for quality engineering* [M]. New York: McGraw-Hill, 1996.
- [19] JEYAPPAUL R, SHAHABUDEEN P, KRISHNAIAH K. Quality management research by considering multi-response problems in the Taguchi method—A review [J]. *The International Journal of Advanced Manufacturing Technology*, 2004, 26: 1331–1337.
- [20] KUMAR P, BARUA P B, GAINDHAR J L. Quality optimization (Multi-Characteristic) through Taguchi's technique and utility concept [J]. *Quality and Reliability Engineering International*, 2000, 16(6): 475–485.
- [21] GAITONDE V N, KARNIK S R, DAVIM J P. Multiperformance optimization in turning of free-machining steel using taguchi method and utility concept [J]. *Journal of Materials Engineering and Performance*, 2008, 18(3): 231–236.
- [22] KIBRIA G, SARKAR B R, PRADHAN B B, BHATTACHARYYA B. Comparative study of different dielectrics for micro-edm performance during microhole machining of Ti–6Al–4V alloy [J]. *International Journal of Advanced Manufacturing Technology*, 2009, 48(5–8): 557–570.
- [23] SINGH K S, KHAMBA J S. High-performance wire electrodes for wire electrical-discharge machining—A review [J]. *Proceedings of the Institution of Mechanical Engineers, Part B: Journal of Engineering Manufacture*, 2012, 226(11): 1757–1773.

TiNi 形状记忆合金的电火花加工性能

M. MANJIAH¹, S. NARENDRANATH¹, S. BASAVARAJAPPA², V. N. GAITONDE³

1. Department of Mechanical Engineering, National Institute of Technology, Surathkal, Karnataka, India;

2. Department of Studies in Mechanical Engineering, University B.D.T. College of Engineering,

Davangere-577 004, Karnataka, India;

3. Department of Industrial and Production Engineering, B. V. B. College of Engineering and Technology,

Hubli-580 031, Karnataka, India

摘要: TiNi 形状记忆合金由于具有优异的超弹性和形状记忆效应等性能而被大量地应用于工业生产中。然而, 形状记忆合金的传统加工相当复杂。因此, 研究 TiNi 形状记忆合金的电火花线切割加工(WEDM)性能。采用 L_{27} 正交阵列以尽量减少实验。在不同的脉冲持续时间、脉冲关断时间、伺服电压、冲洗压力和线速度条件下进行实验。为同步优化提出一种利用 Taguchi 设计与实用理念的多响应优化方法。通过对信噪比(S/N)的均值分析和方差分析, 确定最佳参数水平。Taguchi 分析表明: $1\ \mu\text{s}$ 脉冲持续时间、 $3.8\ \mu\text{s}$ 脉冲关断时间、 $40\ \text{V}$ 伺服电压、 $1.8 \times 10^5\ \text{Pa}$ 冲洗压强和 $8\ \text{m/min}$ 线速度, 有利于同时使材料去除率最大化和表面粗糙度最小化。TiNi 形状记忆合金电火花线切割加工的优化结果表明: 脉冲持续时间显著影响材料去除率和表面粗糙度。在较长的脉冲持续时间时, 在加工表面可观察到放电坑、微裂纹和重铸层。

关键词: TiNi 形状记忆合金; 电火花线切割加工(WEDM); 表面粗糙度; 材料去除率; 表面形貌

(Edited by Chao WANG)